Main Defects of LC-Based $\Sigma\Delta$ Modulators

Ahmed Ashry and Hassan Aboushady

LIP6 Laboratory, University of Pierre and Marie Curie, Paris VI, France.

Email: ahmed.ashry@lip6.fr

Abstract—In this paper, the main defects of LC-based $\Sigma\Delta$ modulators due to process variations are presented. Resonance frequency shift of LC tank circuit, which was discussed is some publications, is shown to be one among many other possible defects that are discussed in this paper. The effect of each defect on modulator output spectrum is shown and discussed. It is suggested that the information extracted from the output spectrum can be used to calibrate the modulator main blocks.

I. INTRODUCTION

Bandpass Continuous-Time (BP CT)$\Sigma\Delta$ modulators that work at RF are considered a promising technique for realizing software defined radio (SDR). They can achieve a reasonable dynamic range by converting only the band of interest around the desired center frequency. Thus, the direct digitization of the RF signal is possible and almost all the signal processing can be done in the flexible and programmable digital domain [1]. LC filters are preferred at RF, as they can achieve higher speed and dynamic range compared to their Gm-C and RC counterparts [2], [3].

One of the main issues in BP CT $\Sigma\Delta$ modulators is the poor accuracy and sensitivity to process variations [4]. Trimming is needed to correct or compensate the drift in circuit components to obtain the optimum performance from the modulator. There are some publications that discuss calibration of CT $\Sigma\Delta$ modulators, but they are limited to calibration of the modulator notch frequency [4]–[6]. In this paper, it is shown that there are more parameters to calibrate other than the notch frequency.

There are several architectures for LC-based $\Sigma\Delta$ modulators. The architecture described in [7] is taken as an example because of its simplicity. The block diagram of the LC-based $\Sigma\Delta$ modulator is shown in Fig. 1, where most of the analog blocks have trimming knobs. This large number of trimming knobs becomes familiar in modern RF design, where it is become more difficult for RF/analog circuits designers to have sufficient margins to tolerate process variations [8].

This large number of trimming knobs gives more flexibility for RF/analog designers, but it makes the calibration process more difficult. The presented work can help in designing a calibration algorithm based on the modulator output spectrum. It can also be useful during design and measurement of the LC-based $\Sigma\Delta$ modulators.

II. TANK CIRCUIT DEFECTS

A. Frequency Shift

The most popular defect of the LC-based modulator is the frequency shift of the tank circuit due to process variations. Fig. 2 shows the effect of frequency shift on the output
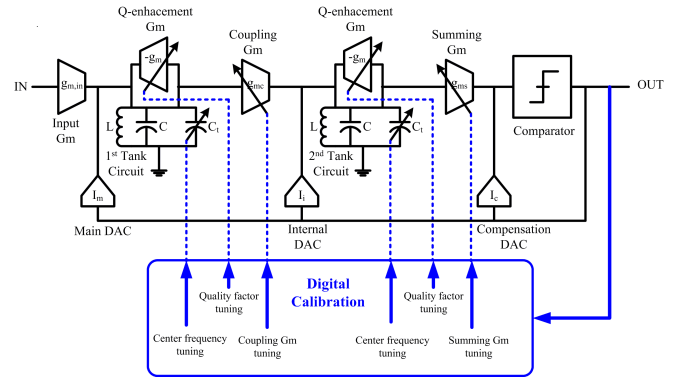

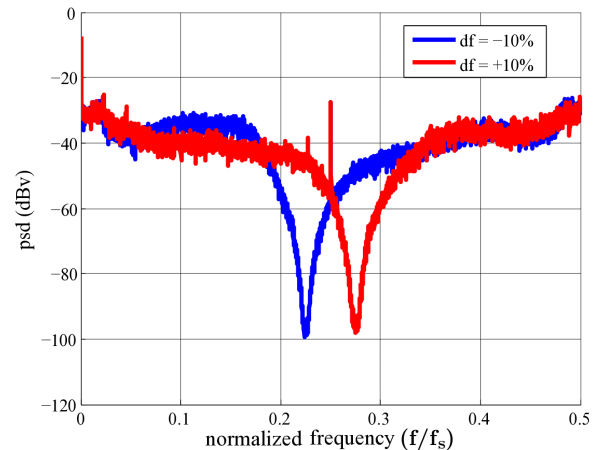Fig. 1. CT $\Sigma\Delta$ modulator with digital calibration

Fig. 2. Frequency shift effect on modulator output spectrum

spectrum of the modulator. The frequency shift of the LC tank circuit can be easily detected, as the notch of the output spectrum is corresponding to the actual resonance frequency of the tank circuit [4]–[6]. However, the detection of the frequency shift can be more difficult if the two tank circuits are not tracking each other, as shown in Fig. 3. The large size of the on-chip conductor makes it difficult to match the two tank circuits, due to large distance separation between them. For this reason, the trimming bits of each tank circuit should be independent to allow for correction of this potential mismatch between the two tank circuits.

B. Quality factor degradation

Quality factor of the on-chip inductor is usually small ($\sim$ 10), which is not sufficient to achieve a reasonable resolution.
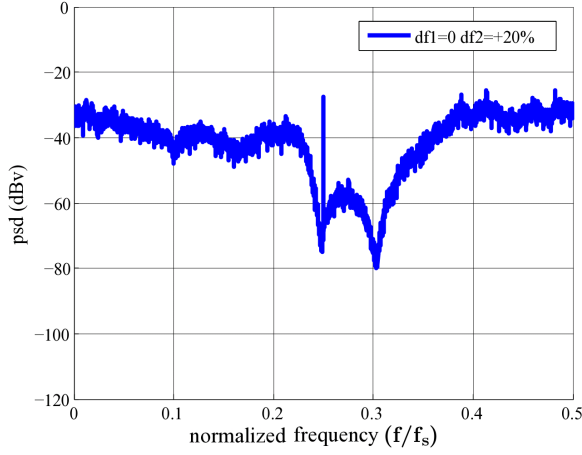
Fig. 3. Frequency shift in a single tank

Fig. 4. Quality factor degradation effect on modulator output spectrum

Quality factor is boosted by using a Q-enhancement transconductor that acts as a negative resistance and cancel the LC tank losses [3]. The enhanced quality factor can obtained from the following equation:

$$Q = Q_o \frac{1}{1 - R_p \, G_q} \tag{1}$$

where Q_o is inductor quality factor, R_p is the inductor effective parallel resistance and G_q is the Q-enhancement transconductor. Due to process variations of both the tank circuit and the transconductor, quality factor can change and make the filter notch less sharp as shown in Fig. 4, where the same degradation occurs in the two tank circuits. It is also possible to get different degradation of quality factor for each tank circuit, as shown in Fig. 5. Thus, trimming is needed for each Q-enhancement transconductor to obtain the highest possible quality factor.

Tuning the transconductor to obtain a very high quality factor seems to be risky, because the tank circuit can become unstable. If the the value of the Q-enhancement transconductor exceeds a certain limit, the positive-feedback loop gain becomes greater than unity, the enhanced quality factor becomes negative as appears from 1, and the filter becomes unstable.

However, the negative feedback of the $\Sigma\Delta$ modulator loop suppresses any oscillation. To validate this assumption, the modulator is simulated with unstable filter as shown in Fig. 6. The SNR curves of the $\Sigma\Delta$ modulator for different positive and negative values of enhanced quality factor are shown in Fig. 7, and the maximum SNR of the modulator versus the quality factor is shown in Fig. 8. It can be deduced from these results, that moving the LC filter to instability region does not affect the overall stability of the $\Sigma\Delta$ modulator. This means that the Q-enhancement transconductor can be freely tuned without worrying about modulator stability.
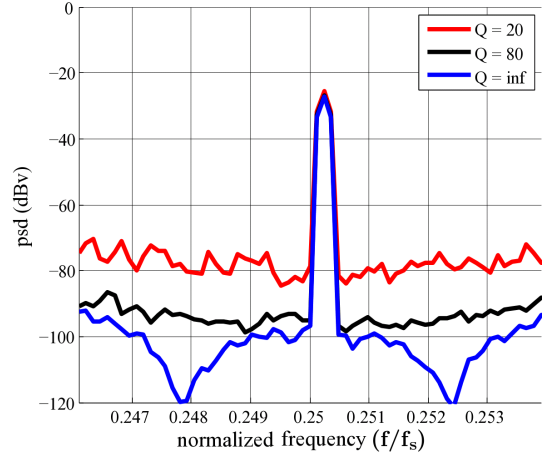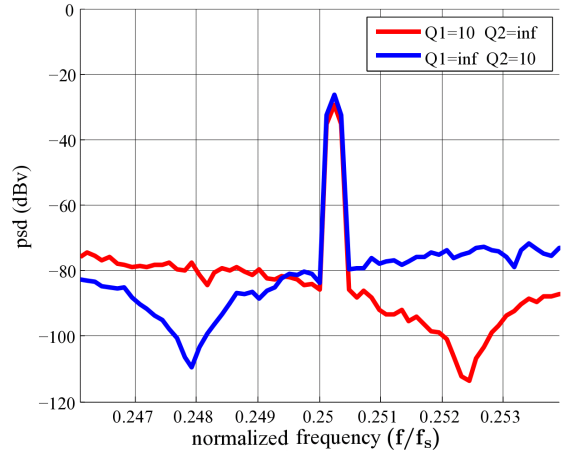

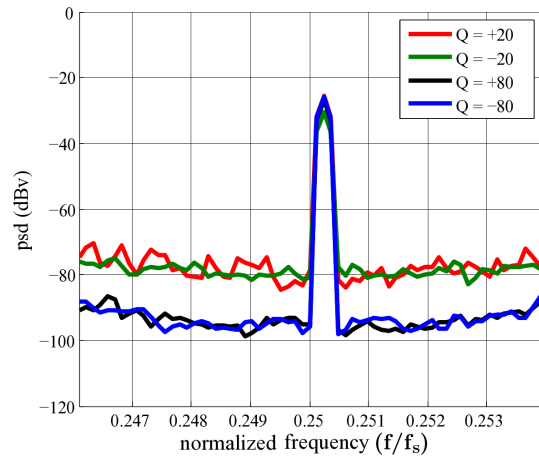Fig. 5. Quality factor degradation in a single tank

Fig. 6. Negative quality factor effect on modulator output spectrum
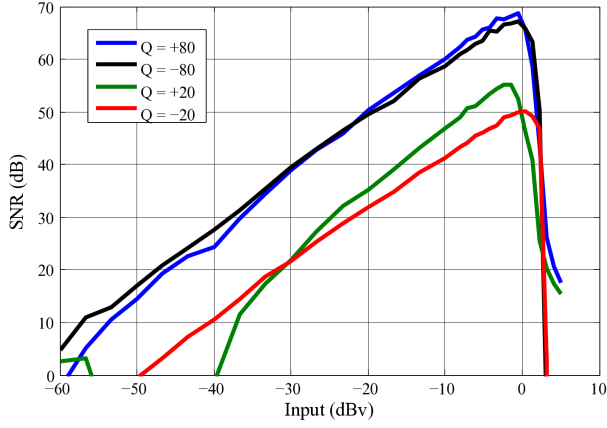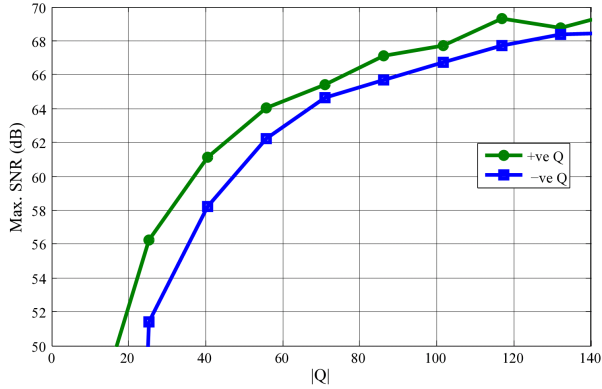
Fig. 7. SNR curves for different quality factor values

Fig. 8. Maximum SNR versus quality factor

III. DAC DEFECTS

A. DAC mismatch

The mismatch between the feedback DAC branches affects the NTF (Noise Transfer Function) of the modulator, and degrades its SNR. Fig 9 and Fig. 10 show the effect of feedback DAC mismatch for internal DAC branch and compensation DAC branch, respectively.

The mismatch between the feedback DAC branches can be minimized by proper layout. However, it is needed to match the feedback DAC current, and the coupling transconductance output current as shown in Fig. 11. This matching difficult to achieve, due to process variations of the tank circuit impedance and the coupling transconductance. For these reason, the coupling transconductance needs to be trimmed to account for these mismatches.

B. DAC gain

For a stable operation of the $\Sigma\Delta$ modulator, the feedback DAC current must be sufficiently larger than the input current. For large input, or for low feedback DAC current, the stability of the modulator degrades and the signal band is filled with undesired tones that degrades the modulator SNR as shown in Fig. 12. This defect can be controlled be either trimming the DAC current or the input transconductor.
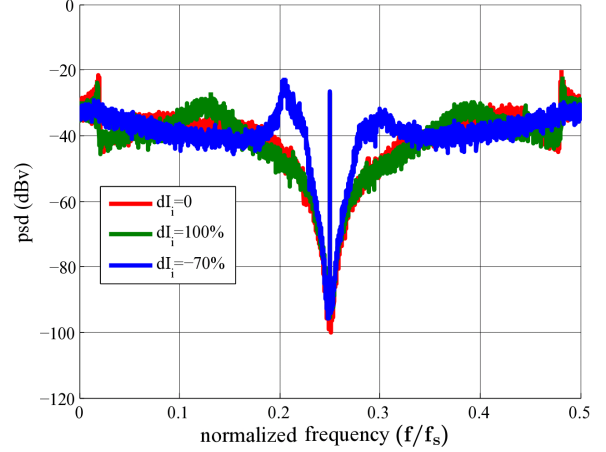

Fig. 9. Internal DAC mismatch effect on modulator output spectrum
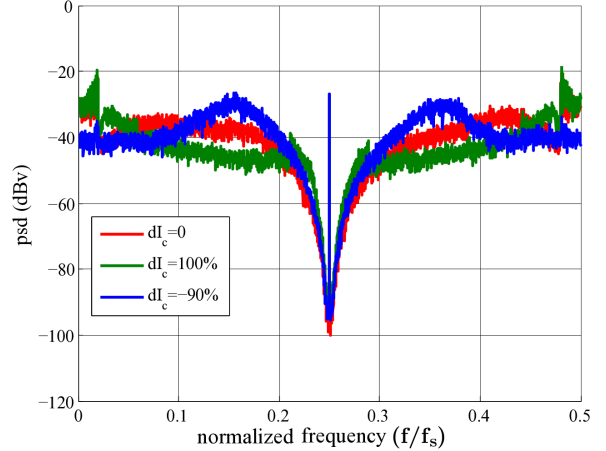

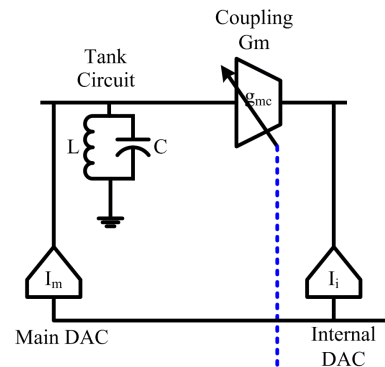Fig. 10. Compensation DAC mismatch effect on modulator output spectrum
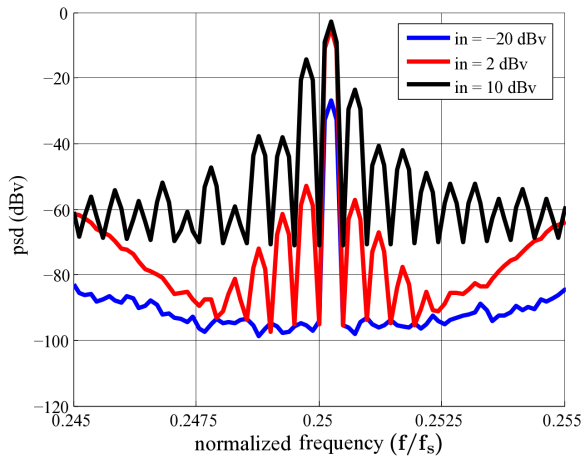

Fig. 11. DAC mismatch reason

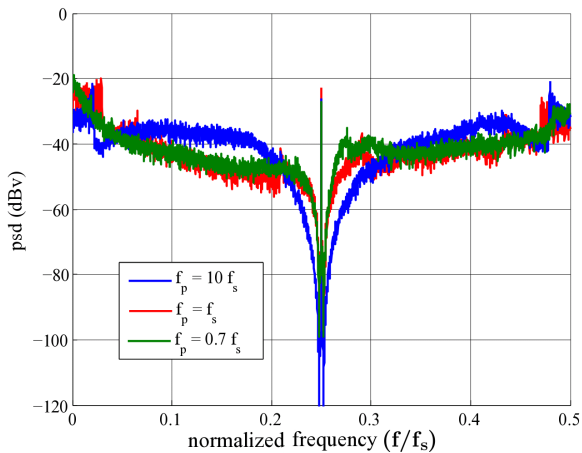Fig. 12.   Effect of high input current relative to the feedback DAC current

Fig. 13.   Effect of summing node lowpass filter

IV. CONCLUSION

The main defects of the LC-based CT $\Sigma\Delta$Ms were presented. The effect of each defect on the modulator output spectrum and SNR is discussed. Most of the defect have a unique effect on the output spectrum that can be detected and compensated by proper trimming. These results can be useful in design and measurement phases, and can be used to implement a digital calibration algorithm.

REFERENCES

[1] N. Beilleau, H. Aboushady, F. Montaudon, and A. Cathelin, "A 1.3V 26mW 3.2Gs/s undersampled LC bandpass $\Sigma\Delta$ ADC for a SDR ISM-band receiver in 130nm CMOS," in *Proc. IEEE Radio Frequency Integrated Circuits Symposium, (RFIC'09)*, June 2009, pp. 383–386.

[2] T. Kaplan, J. Cruz-Albrecht, M. Mokhtari, D. Matthews, J. Jensen, and M. Chang, "A 1.3-GHz IF digitizer using a 4th-order continuous-time bandpass $\Sigma\Delta$ modulator," in *Proc. IEEE Custom Integrated Circuits Conference, (CICC'03)*, Sept. 2003, pp. 127–130.

[3] B. K. Thandri and J. Silva-Martinez, "A 63 dB SNR, 75-mW bandpass RF $\Sigma\Delta$ ADC at 950 MHz using 3.8-GHz clock in 0.25-μm SiGe BiCMOS technology," *IEEE J. Solid-State Circuits*, vol. 42, no. 2, pp. 269–279, Feb. 2007.

[4] F. Silva-Rivas, C.-Y. Lu, P. Kode, B. K. Thandri, and J. Silva-Martinez, "Digital based calibration technique for continuous-time bandpass sigma-delta analog-to-digital converters," *Analog Integrated Circuits and Signal Processing*, vol. 59, pp. 91–95, Apr. 2009.

[5] Y.-S. Shu, B.-S. Song, and K. Bacrania, "A 65nm CMOS CT $\Sigma\Delta$ modulator with 81dB DR and 8MHz BW auto-tuned by pulse injection," in *Digest of Tech. Papers IEEE International Solid-State Circuits Conference , (ISSCC'08)*, Feb. 2008, pp. 500–631.

[6] H. Huang and E. Lee, "A 1.2V direct background digital tuned continuous-time bandpass sigma-delta modulator," in *Proc. European Solid-State Circuits Conference, (ESSCIRC'01)*, Sept. 2001, pp. 526–529.

[7] A. Ashry and H. Aboushady, "Using excess loop delay to simplify LC-based $\Sigma\Delta$ modulators," *Electronics Letters*, vol. 45, no. 25, pp. 1298–1299, Dec. 2009.

[8] R. Staszewski, R. B. Staszewski, T. Jung, T. Murphy, I. Bashir, O. Eliezer, K. Muhammad, and M. Entezari, "Software assisted digital RF processor (DRP^{TM}) for single-chip GSM radio in 90 nm CMOS," *IEEE J. Solid-State Circuits*, vol. 45, no. 2, pp. 276–288, Feb. 2010.

C. Summing node

The delay compensation feedback DAC branch current is added to the coupling transconductance output current, and converted to voltage using a resistor. The resistor and the parasitic capacitance at this summation node creates a lowpass filter and adds undesired pole to the loop filter. The cut-off frequency of this lowpass filter has to be kept far from the LC filter center frequency to avoid degrading the modulator stability. Fig. 13 shows the effect of this lowpass filter on the output spectrum of the modulator for different values of the cut-off frequency.